applied sciences

MDPI

Article

Oxadiazolyl-Pyridinium as Cationic Scaffold for Fluorinated Ionic Liquid Crystals †

Melina S. Weber [1,2], Margit Schulze [3], Giuseppe Lazzara [4], Antonio Palumbo Piccionello [1], Andrea Pace [1] and Ivana Pibiri [1,*]

1 Dipartimento di Scienze e Tecnologie Biologiche, Chimiche e Farmaceutiche (STEBICEF), University of Palermo, Viale delle Scienze, Ed. 17, 90128 Palermo, Italy; Melina.weber@uni-bayreuth.de (M.S.W.); antonio.palumbopiccionello@unipa.it (A.P.P.); andrea.pace@unipa.it (A.P.)
2 Macromolecular Chemistry I, University of Bayreuth, Universitätsstraße 30, 95447 Bayreuth, Germany
3 Department of Natural Sciences, Bonn-Rhein-Sieg University of Applied Sciences, von-Liebig-Straße 20, 53359 Rheinbach, Germany; margit.schulze@h-brs.de
4 Dipartimento di Fisica e Chimica (DiFC), University of Palermo, Viale delle Scienze, Ed. 17, 90128 Palermo, Italy; giuseppe.lazzara@unipa.it
* Correspondence: ivana.pibiri@unipa.it; Tel.: +39-091-23897545
† This work is dedicated to the memory of Prof. Sergio Rosselli.

Featured Application: Fluorinated ionic liquid crystals, due to their easy synthetic modulation, inertness, and potential as quasi solid-state electrolytes, can find perspective application in DSSCs solar cells, but also in many other electronic and optoelectronic devices, such as supercapacitors, smart windows, and lithium batteries.

Abstract: The synthesis and characterization of a new class of 1,2,4-oxadiazolylpyridinium as a cationic scaffold for fluorinated ionic liquid crystals is herein described. A series of 12 fluorinated heterocyclic salts based on a 1,2,4-oxadiazole moiety, connected through its C(5) or C(3) to an *N*-alkylpyridinium unit and a perfluoroheptyl chain, differing in the length of the alkyl chain and counterions, has been synthesized. As counterions iodide, bromide and bis(trifluoromethane)sulfonimide have been considered. The synthesis, structure, and liquid crystalline properties of these compounds are discussed on the basis of the tuned structural variables. The thermotropic properties of this series of salts have been investigated by differential scanning calorimetry and polarized optical microscopy. The results showed the existence of an enantiotropic mesomorphic smectic liquid crystalline phase for six bis(trifluoromethane)sulfonimide salts.

Keywords: ionic liquids; liquid crystals; fluorinated salts; heterocyclic; mesogens

Citation: Weber, M.S.; Schulze, M.; Lazzara, G.; Palumbo Piccionello, A.; Pace, A.; Pibiri, I. Oxadiazolyl-Pyridinium as Cationic Scaffold for Fluorinated Ionic Liquid Crystals. *Appl. Sci.* **2021**, *11*, 10347. https://doi.org/10.3390/app112110347

Academic Editors: Eric Guibal and Roberto Zivieri

Received: 23 September 2021
Accepted: 31 October 2021
Published: 3 November 2021

1. Introduction

Liquid crystals (LCs) can be described as the matter between the isotropic liquid and the anisotropic solid crystal. The liquid crystalline phase possesses some of the characteristics of the order found in the solid crystal as well as some of the disorder existing in liquids and is often referred to as mesophase [1]. Ionic liquids (ILs) are salts which consist of organic cations paired with a variety of anions and melt at low temperatures, usually below 100 °C [2,3]. When a liquid crystalline material consists of anion and cations, it is called an ionic liquid crystal (ILC) [4]. Due to the ionic character and the ability to form liquid crystalline phases with structural and sometimes even positional order, the combined properties of ionic liquids and liquid crystals makes the ionic liquid crystals highly attractive for a variety of applications such as ion-conductive materials in batteries [5,6] or dye-sensitized solar cells [7]. The physical properties of IL and ILCs can be tailored by judicious selection of the central core, such as heterocycles, the substituents and their position, the introduction of alkyl chains and fluorinated moieties of various length as well as the right choice

of the counterion [4,8]. In this context, a variety of 1,2,4-oxadiazoles and 1,2,4-triazoles have been investigated with tuned structural variables [3,8–13]. The latest studies have focused on a series of 1,2,4-triazolium ions with chain length variation of the attached fluoroalkyl (m = 3, 7, 9) and alkyl chains (n = 10, 12, 14) as well as different counterions such as trifluoromethanesulfonate ([OTf^-]), bis(trifluoromethane)sulfonimide ([Tf_2N^-]), and tetrafluoroborate ([BF_4^-]). This family is proposed as thermotropic triphilic ionic liquid crystals, showing predominantly smectic A (SmA) phases, which can be dominantly attributed to the ionic nature of these materials as well as to the alkyl and perfluoroalkyl chains [10,14–17]. Compared to this family, the perfluoroheptyl 1,2,4-oxadiazoles bearing a *N*-methylated-4-pyridyl moiety (visualized in Chart 1) with iodide [I^-] or [OTf^-] as counterions behave as ionic liquids, thus, being low-melting organic salts. However, the *N*-methylated-3-pyridyl moiety has been found to exhibit thermally induced liquid crystalline behavior [10]. In order to drive 1,2,4-oxadiazoles with the 4-substituted pyridinium to LC formation, the combination of perfluoroheptyl chains and the introduction of long alkyl chains into the system are a promising way to obtain micro-segregation resulting in ionic liquid crystalline behavior. Thus, we focused on the synthesis and characterization of a new class of 1,2,4-oxadiazolylpyridinium salts as cationic scaffold for fluorinated ionic liquid crystals. The 12 salts of this work are summarized in Chart 1 and differ in the reciprocal position of the perfluoroheptyl chain and the pyridinium moieties on the interspacing oxadiazole ring, resulting in **1a-f** and **2a-f** being regioisomers. Furthermore, alkyl chains of different length ($C_{10}H_{21}$ for **1a**,**d** and **2a**,**d**; $C_{12}H_{25}$ for **1b**,**e** and **2b**,**e**; $C_{14}H_{29}$ for **1c**,**f** and **2c**,**f**) are inserted into the system. Additionally, iodide [I^-], bromide [Br^-] or bis(trifluoromethane)sulfonimide [Tf_2N^-] are considered as counterions. The synthesis, metathesis, structure, and liquid crystalline properties of these compounds are discussed on the basis of the tuned structural variables. The thermotropic properties of this series of salts have been investigated by a combination of differential scanning calorimetry and polarized optical microscopy.

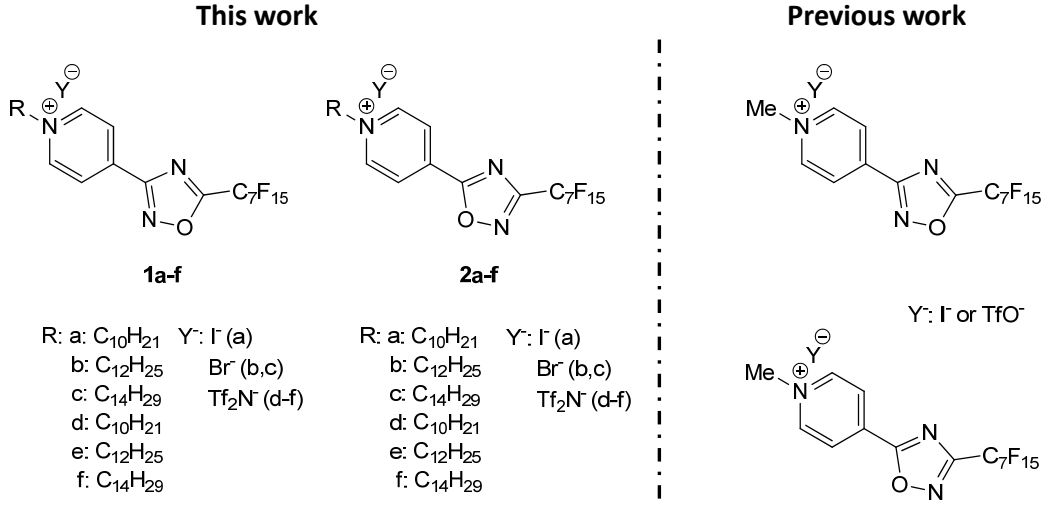

Chart 1. Structures of the 12 perfluoroheptyl 1,2,4-oxadiazolylpyridinium salts **1a-f** and **2a-f** investigated in this work and the perfluoroheptyl 1,2,4-oxadiazolyl *N*-methylpyridinium salts reported in previous work [9,10].

2. Materials and Methods

2.1. General

^{1}H-NMR spectra were recorded on a Bruker AC 250 E spectrometer using chloroform-*d* (99.80%, VWR Chemicals) ($CDCl_3$) or acetonitrile-d_3 (99.80% VWR Chemicals) (CD_3CN) solutions.

Reversed Phase HPLC/ESI/Q-TOF HRMS experiments: Water and acetonitrile were of HPLC/MS grade. Formic acid was of analytical quality. The HPLC system was an

Agilent 1260 Infinity. A reversed-phase C18 column (ZORBAX Extended-C18 2.1 × 50 mm, 1.8 µm) with a Phenomenex C18 security guard column (4 mm × 3 mm) was used. The flow rate was 0.4 mL/min and the column temperature was set to 30 °C. The eluents were formic acid-water (0.1:99.9, v/v) (phase A) and formic acid-acetonitrile (0.1:99.9, v/v) (phase B). The following gradient was employed: 0–10 min, linear gradient from 5% to 95% B; 10–15 min, washing and reconditioning of the column to 5% B. The injection volume was 10 µL. The eluate was monitored through MS TIC. Mass spectra were obtained on an Agilent 6540 UHD accurate-mass Q-TOF spectrometer equipped with a Dual AJS ESI source working in positive mode. N2 was employed as desolvation gas at 300 °C and a flow rate of 9 L/min. The nebulizer was set to 45 psi. The Sheath gas temperature was set at 350 °C and a flow of 12 L/min. A potential of 3.5 kV was used on the capillary for positive ion mode. The fragmentor was set to 175 V. MS spectra were recorded in the 150–1000 m/z range.

Polarized optical microscopy (POM) analysis of the compounds were carried out by a Zeiss Axioskop 40Pol microscope equipped with a Linkham hot-stage and a Mettler FP90 central processor to control the temperature. The analysis was performed with the samples placed between a glass slide and a cover slip. The samples were heated and cooled with a rate of 10 °C min^{-1}. An InfinityX-21 MP digital camera mounted atop the microscope allows to capture photomicrographs. Images were recorded at magnifications of 100× or 200× and cross-polarized light.

Differential scanning calorimetry (DSC) measurements were carried out with a TA Instruments mod. 2920 Differential Scanning Calorimeter with a TA Instruments Refrigerated Cooling System. Samples were prepared in aluminum TA Tzero Hermetic Pans and Lids (T121019, T121106, made in Switzerland) using SCALTEC (d = 0.01/0.1 mg) as the analytical balance. The sample size was of the order of 4 mg for each sample. The analysis was carried out with heating and cooling rates of 10 °C min^{-1} for every sample under a N_2 flux of 60 cm^3 min^{-1}. Seven ramps were included in the temperature program: one heating step from room temperature to high temperatures until isotropization of the sample at 10 °C min^{-1}, followed by a cooling step to −30 °C and by the other analogous heating/cooling cycles. The repetition of the same ramps was done to assess the reproducibility of the phase transitions. Due to the Dual Sample Cell, two samples with equal melting points were measured at the same time.

2.2. Synthesis

2.2.1. Synthesis of Perfluoroheptyl 1,2,4-Oxadiazolylpyridines **1** and **2**

The 1,2,4-oxadiazole precursor 5-(perfluoroheptyl)-3-(pyridin-4-yl)-1,2,4-oxadiazole (**1**) and its regioisomer 3-(perfluoroheptyl)-5-(pyridin-4-yl)-1,2,4-oxadiazole (**2**) have been prepared as published elsewhere following the classical methodology for the synthesis of 1,2,4-oxadiazoles and the ANRORC (Addition of a Nucleophile with Ring Opening and Ring Closure) rearrangement, respectively [18–20]. This includes the reaction of *N*′-Hydroxyisonicotinimidamide with perfluorooctanoyl chloride (97%, Sigma-Aldrich, Milan, Italy) to obtain compound **1** and an ANRORC rearrangement of compound **1** into the regioisomer **2**.

5-(perfluoroheptyl)-3-(pyridin-4-yl)-1,2,4-oxadiazole 1: White solid. Yield: 48%. ^{1}H-NMR (300 MHz, CD_3CN) δ: 8.86 (d, J = 4.6 Hz, 2H, Ar), 8.00 (d, J = 4.6 Hz, 2H, Ar).

3-(perfluoroheptyl)-5-(pyridin-4-yl)-1,2,4-oxadiazole 2: White solid. Yield: 86%. ^{1}H-NMR (300 MHz, CD_3CN) δ: 8.93 (d, J = 6.0 Hz, 2H, Ar), 8.05 (d, J = 6.1 Hz, 2H, Ar).

2.2.2. Synthesis of Perfluoroheptyl 1,2,4-Oxadiazolylpyridinium Salts **1a-c** and **2a-c**

The salts **1a-c** and **2a-c** were synthesized according to Scheme 1 by 5-(Perfluoroheptyl)-3-(pyridin-4-yl)-1,2,4-oxadiazole (**1**) or 3-(Perfluoroheptyl)-5-(pyridin-4-yl)-1,2,4-oxadiazole (**2**) (100 mg, 0.1941 mmol) in acetonitrile (5 mL, Sigma-Aldrich, St. Louis, MO, USA) and by subsequent addition of 5 mole eq. 1-iododecane (98%, Sigma-Aldrich) (**1a**, **2a**), 1-bromododecane (97%, Sigma-Aldrich, St. Louis, MO, USA) (**1b**, **2b**) or 1-bromotetradecane

(97%, Sigma-Aldrich, St. Louis, MO, USA) (**1c**, **2c**), respectively. The mixture was stirred in an oil bath for one week at 80 °C. The reaction was monitored by TLC (petroleum ether and ethyl acetate 2:1 (Sigma-Aldrich and 99.9% VWR-Chemicals, respectively)). After cooling, the mixture was dried under vacuum. Impurities were extracted with petroleum ether (Sigma-Aldrich, St. Louis, MO, USA) several times and the product was dried under vacuum. Dissolving in acetonitrile (Sigma-Aldrich, St. Louis, MO, USA) and drying under vacuum yielded the desired products.

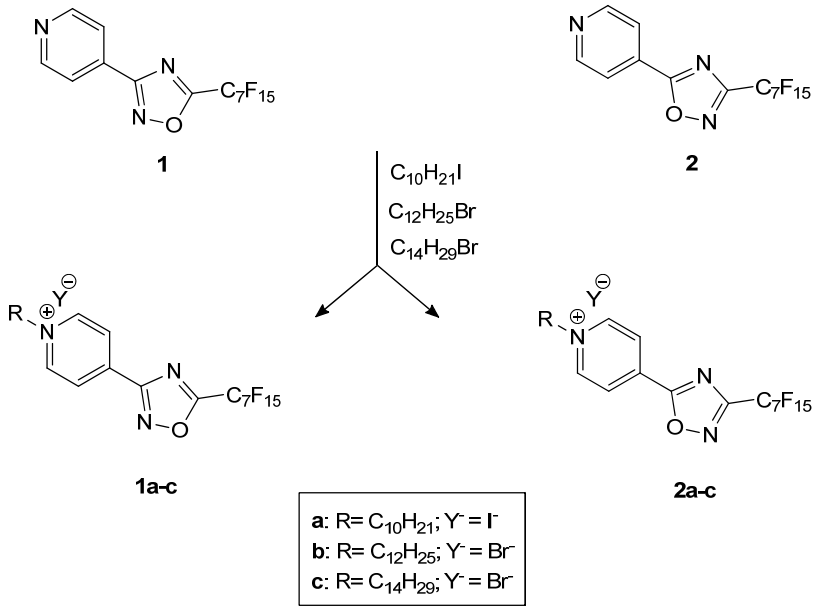

Scheme 1. Synthesis of perfluoroheptyl 1,2,4-oxadiazolylpyridinium salts **1a-c** and **2a-c** from the regioisomers perfluoroheptyl 1,2,4-oxadiazolylpyridines **1** and **2**.

1-decyl-4-(5-(perfluoroheptyl)-1,2,4-oxadiazol-3-yl) pyridin-1-ium iodide (1a): Orange solid. Yield: 88%. ^{1}H-NMR (300 MHz, CD_3CN) δ: 8.96 (d, J = 6.8 Hz, 2H, Ar), 8.64 (d, J = 6.2 Hz, 2H, Ar), 4.64 (t, J = 7.7 Hz, 2H), 1.34 (m, 16H), 0.89 (t, J = 7 Hz, 3H). MS analysis: Calc.: 656.1752 g mol^{-1}, exp.: 656.1759 g mol^{-1}.

1-dodecyl-4-(5-(perfluoroheptyl)-1,2,4-oxadiazol-3-yl) pyridin-1-ium bromide (1b): White solid. Yield: 77%. ^{1}H-NMR (300 MHz, $CDCl_3$) δ: 9.75 (d, J = 5.9 Hz, 2H, Ar), 8.70 (d, J = 5.8 Hz, 2H, Ar), 5.20 (t, J = 7.2 Hz, 2H), 2.11 (q, 2H), 1.32 (m, 18H), 0.89 (t, J = 6.0 Hz, 3H). MS analysis: Calc.: 684.2065 g mol^{-1}, exp.: 684.2042 g mol^{-1}.

1-tetradecyl-4-(5-(perfluoroheptyl)-1,2,4-oxadiazol-3-yl) pyridin-1-ium bromide (1c): White solid. Yield: 63%. ^{1}H-NMR (300 MHz, $CDCl_3$) δ: 9.74 (d, J = 6.4 Hz, 2H, Ar), 8.69 (d, 2H, J = 6.9 Hz, Ar), 5.18 (t, J = 7.3 Hz, 2H), 2.09 (q, J = 7 Hz, 2H), 1.31 (m, 22H), 0.89 (t, J = 6.5 Hz, 3H). MS analysis: Calc.: 712.2378 g mol^{-1}, exp.: 712. 2370 g mol^{-1}.

1-decyl-4-(3-(perfluoroheptyl)-1,2,4-oxadiazol-5-yl) pyridin-1-ium iodide (2a): Orange/red solid. Yield: 93%. ^{1}H-NMR (300 MHz, $CDCl_3$) δ: 9.75 (d, J = 6.5 Hz, 2H, Ar), 8.78 (d, J = 6.6 Hz, 2H, Ar), 5.09 (t, J = 7.5 Hz, 2H), 1.32 (m, 16H), 0.88 (t, J = 6.6 Hz, 3H). MS analysis: Calc.: 656.1752 g mol^{-1}, exp.: 656.1764 g mol^{-1}.

1-dodecyl-4-(3-(perfluoroheptyl)-1,2,4-oxadiazol-5-yl) pyridin-1-ium bromide (2b): White solid. Yield: 63%. ^{1}H-NMR (300 MHz, CD_3CN) δ: 9.80 (d, J = 6.6 Hz, 2H, Ar), 8.73 (d, J = 6.5 Hz, 2H, Ar), 5.19 (t, J = 7.4 Hz, 2H), 2.12 (q, 2H), 1.26 (m, 20H), 0.89 (t, J = 6.6 Hz, 3H). MS analysis: Calc.: 684.2065 g mol^{-1}, exp.: 684.2045 g mol^{-1}.

1-tetradecyl-4-(3-(perfluoroheptyl)-1,2,4-oxadiazol-5-yl) pyridin-1-ium bromide (2c): White solid. Yield: 49%. ^{1}H-NMR (300 MHz, CD_3CN) δ: 9.80 (d, J = 5.9 Hz, 2H, Ar), 8.74 (d, J = 6.1 Hz, 2H, Ar), 5.20 (t, J = 7.3 Hz, 2H), 1.26 (m, 24H), 0.88 (br s, -). MS analysis: Calc.: 712.2378 g mol^{-1}, exp.: 712. 2374 g mol^{-1}.

2.2.3. Metathesis to **1d-f** and **2d-f** with Bis(trifluoromethane)sulfonimide as Counterion

The ion exchange of the precursor salts was conducted as described in Scheme 2. Therefore, the salts **1a′-c** or **2a-c** were separately dissolved in a minimum amount of methanol (VWR-Chemicals) (3–10 mL) and bis(trifluoromethane)sulfonimide lithium salt (97%, Sigma-Aldrich) (5 mole eq.) was added. The mixture was heated up to 30–35 °C and stirred for 0.5 h. Water was added dropwise until a permanent precipitate was formed. The mixture was stirred for 1 h. The solid was filtered under vacuum and washed with water.

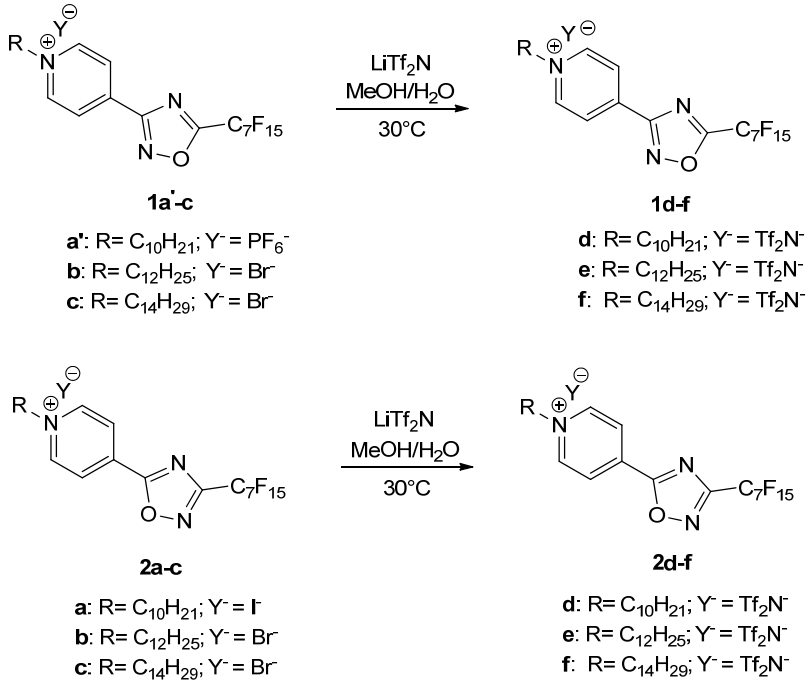

Scheme 2. Synthesis of the perfluoroheptyl 1,2,4-oxadiazolylpyridinium salts **1d-f** and **2d-f** from the precursor salts **1a′-c** and **2a-c**.

1-decyl-4-(5-(perfluoroheptyl)-1,2,4-oxadiazol-3-yl) pyridin-1-ium bis(trifluoromethane) sulfonimide (1d): White solid. Yield: not recorded. MS analysis: Calc.: 279.9178 g mol^{-1}, exp.: 279.9192 g mol^{-1}.

1-dodecyl-4-(5-(perfluoroheptyl)-1,2,4-oxadiazol-3-yl) pyridin-1-ium bis(trifluormethane) sulfonimide (1e): White solid. Yield: 76%. MS analysis: Calc.: 279.9178 g mol^{-1}, exp.: 279.9193 g mol^{-1}.

1-tetradecyl-4-(5-(perfluoroheptyl)-1,2,4-oxadiazol-3-yl) pyridin-1-ium bis(trifluoromethane) sulfonimide (1f): White solid. Yield: 83%. MS analysis: Calc.: 279.9178 g mol^{-1}, exp.: 279.9193 g mol^{-1}.

1-decyl-4-(3-(perfluoroheptyl)-1,2,4-oxadiazol-5-yl) pyridin-1-ium bis(trifluoromethane) sulfonimide (2d): White solid. Yield: 74%. MS analysis: Calc.: 279.9178 g mol^{-1}, exp.: 279.9204 g mol^{-1}.

1-dodecyl-4-(3-(perfluoroheptyl)-1,2,4-oxadiazol-5-yl) pyridin-1-ium bis(trifluoromethane) sulfonimide (2e): White solid. Yield: 56%. MS analysis: Calc.: 279.9178 g mol^{-1}, exp.: 279.9192 g mol^{-1}.

1-tetradecyl-4-(3-(perfluoroheptyl)-1,2,4-oxadiazol-5-yl) pyridin-1-ium bis(trifluoromethane) sulfonimide (2f): White solid. Yield: 46%. MS analysis: Calc.: 279.9178 g mol^{-1}, exp.: 279.9203 g mol^{-1}.

3. Results and Discussion

3.1. Synthesis

The perfluoroheptyl 1,2,4-oxadiazolylpyridine precursor (**1**) has been synthesized following the classical methodology of the amidoxime route (Yield = 48%) [18,19]. The

regioisomer (**2**) with the reciprocal position of the perfluoroheptyl chain and the 4-pyridyl group with respect to the heteroaromatic core has been prepared according to the ANRORC method with a yield of 86% [20]. The quaternization reactions of these precursors have been carried out to obtain the series of perfluoroheptyl 1,2,4-oxadiazolylpyridinium salts (**1a-c** and **2a-c**) by direct alkylation in acetonitrile with suitable alkylating agents. For this, 1-iododecane, 1-bromododecane and 1-bromotetradecane have been chosen. The success of the quaternization at the pyridine nitrogen of compounds **1** and **2** towards **1a-c** and **2a-c** (Scheme 1) was assessed by ^{1}H-NMR (reported in the SI) and mass spectrometry (MS). Yields up to 93% have been obtained of the desired products. The metathesis from **1a′-c** and **2a-c** with iodide and bromide or hexafluorophosphate (**1a′**, synthesis and analytical data reported in the SI, Figure S9) as counter ions has been realized in methanol and addition of the new desired counterion, here bis(trifluoromethane)sulfonimide lithium salt. Filtration and washing with water yielded the desired products **1d-f** and **2d-f** (Scheme 2). Detection of the new counterion bis(trifluoromethane)sulfonimide ([Tf_2N^-]) has been done via HPLC-MS in a negative mode. Complete conversion from iodide/bromide/hexafluorophosphate to [Tf_2N^-] has been guaranteed by HPLC-MS as no residues of the precursor counterions were detected.

3.2. Thermotropic Liquid Crystalline Phase Behavior

The thermotropic liquid crystalline phase behavior of the salts has been characterized using a combination of differential scanning calorimetry (DSC) and polarized optical microscopy (POM). The DSC analyses were conducted at first to obtain a clear picture about the thermal behavior of the samples. Afterwards, POM was used to examine the samples very carefully to determine the mesophase types exhibited by the samples. Starting with the precursor perfluoroheptyl 1,2,4-oxadiazolylpyridium salts with iodide or bromide as counterion, the melting points for **1a-c** and **2b-c** could not be determined in the DSC traces, indicating decomposition before melting—except for sample 2a. Furthermore, no melting points were observed during the POM analyses, indicating that these salts decompose at temperatures higher than 200 °C. In the previous study about the salts containing 1,2,4-oxadiazole connected through its C(5) or C(3) to an *N*-methylated 4-pyridyl moiety and a perfluoroheptyl chain, a demethylation reaction was experimentally observed, which is likely through a retro S_N2 mechanism [10]. Similarly, this has been reported for imidazolium halides and could justify the instability at higher temperatures of the alkylated salts **1a-c** and **2b-c** having iodide and bromide as counterion [21]. Only the salt **2a** with iodide as the counter ion possesses an ionic liquid crystalline phase behavior in the POM analysis as well as in the DSC traces. However, this is not further discussed as the halide salts are considered as precursors for the preparation of ILCs observed by following metathesis due to the envisaged LC properties. In fact, the alkylation with alkyl halides is efficient and feasible to obtain the precursors salts, since the halides act as good leaving groups. Importantly, the metathesis resulting in [Tf_2N^-] as the counterion is necessary to lower the melting point of the salts and stress the structure in order to observe ionic liquid crystalline phase behavior. In our preliminary metathesis experiments with different counterions such as hexafluorophosphate, we did not detect in any case ionic liquid or liquid crystal behavior. We observed thermal degradation of the samples, and this observation lead us to exclude those different counterions from this study set.

A possible explanation for the thermal instability could be related to the coordinating ability of the anion: the decomposition temperature is following the order of Cl^- < [BF_4^-] ~ [PF_6^-] < [Tf_2N^-], which is inversely proportional to the tendency to form a stable alkyl-X species. Moreover, increasing the anion size reduces the Coulombic attraction contributions to the lattice energy of the crystal, which leads to lower melting points and explains the choice of the bigger anion [Tf_2N^-] [22]. After the metathesis, the six salts **1d-f** and **2d-f** with [Tf_2N^-] as the counterion were investigated by means of DSC. While the precursor salts, except of **2a**, were identified as not mesomorphic, the DSC traces for all salts with [Tf_2N^-] as the counterion show relevant events on heating (endotherm) and cooling (exotherm) as

shown in the second heating and cooling cycle for all six salts in Figure 1. All salts possess, at least, three reversible transitions in the cooling and heating cycles. Concentrating on the cooling cycles, three relevant events are observed for each salt, whereby the second transition seems to be the most pronounced. Considering the temperatures of the second transition, they seem not to shift drastically within each of the salt series **1d-f** and **2d-f.** The temperatures of the first and third transition instead shift to higher temperatures for the longer alkyl chain within the series. Concentrating on the heating cycles, at least three transitions can be observed for all salts and some of the salts (**1d**, **1f**, **2e**, **2f**) show an additional transition at lower temperatures. The second transition is the most pronounced and does not shift much in temperature within the series. In contrast, the first and third transition shifts to higher temperatures with the increasing alkyl chain within the series. A small hysteresis is visible for all salts comparing the cooling and heating transitions.

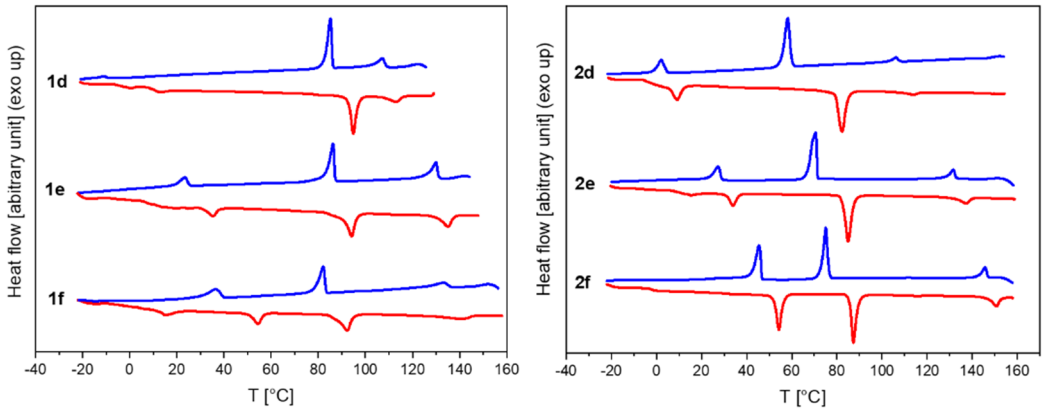

Figure 1. Differential scanning calorimetry (DSC) recorded for **1d-f** and **2d-f** showing the second cooling and heating curves with 10 °C min^{-1} under nitrogen atmosphere. Exothermic peaks point upward.

As these salts exhibit several transitions upon heating and cooling, it is reasonable to assume that they show at least one liquid crystalline phase. Thus, the first transition within the cooling cycle after heating for all salts is identified as the clearing point (T_c) from the isotropic melt into the mesophase and the subsequent transition as the melting point (T_m). The clearing and melting points are summarized in Table 1. Based on this data, an increase of the clearing points (the first transition) within each series of the 3-pyridinium salts (**1d-f**) and the 5-pyridinium derivatives (**2d-f**) is observed. Thus, increasing clearing points with increasing chain length are observed and could be explained by attractive van der Waals forces and the interactions between the hydrocarbon chains contributing to the local structure and thus, inducing micro-segregation between hydrophobic alkyl chains and charged ionic regions [22]. Besides this trend, by comparing the regioisomers with each other when bearing the same alkyl chain length, the clearing points are quite similar. Only the salts **1f** and **2f** differ in order of ~14 °C. On the other hand, the melting points (the second transitions) are quite similar within the series (except for **2d**) but differ depending of the reciprocal position of the perfluoroheptyl chain and the pyridinium moieties on the interspacing oxadiazole ring. In fact, the 3-pyridinium salts (**1d-f**) possess higher melting points than the corresponding 5-pyridinium derivatives.

The following discussion about the liquid crystalline phase behavior will concentrate only on the transitions upon cooling. For this, the temperature of each transition, the corresponding enthalpy values and the suggested phase transitions are summarized in Table 2. Since the change in structural ordering of the phase is proportional to the magnitude of the enthalpy change, the enthalpies in Table 2 can be compared with literature values to determine the type of phase. The enthalpy for the melting transition from a crystalline solid-state to a liquid crystalline phase (Cr ⟶ LC) or an isotropic liquid (Cr ⟶ I) phase is ~30 to 50 kJ mol^{-1}, whereas the enthalpy for a liquid crystalline phase to a liquid crystalline

phase (LC ⟶ LC) and a liquid crystalline phase to an isotropic liquid (LC ⟶ I) are only associated with small changes around ~4–6 kJ mol^{-1} [23].

Table 1. Clearing [T_c] and Melting [T_m] points of the salts **1d-f** and **2d-f** with [Tf_2N^-] as the counterion extracted from the second cooling cycle from the DSC curves.

Salt	Clearing Points T_c [°C]	Melting Points T_m [°C]
1d	108.8	86.1
1e	131.0	87.1
1f	133.0	82.0
2d	107.9	60.0
2e	132.8	71.4
2f	146.9	76.5

Table 2. Transition temperatures (T), enthalpies (△H) and the phase transition of the salts **1d-f** and **2d-f** obtained from the DSC traces upon cooling with 10 °C min^{-1}.

Salt	T [°C] [a]	△H [kJ mol^{-1}]	Transition
1d	108.8	4.2	Iso–LC (SmA)
	86.1	15.1	LC (SmA)–Cr″
	−10.9	-	Cr″–Cr′
1e	131.0	8.7	Iso–LC (SmA)
	87.1	15.3	LC (SmA)–Cr″
	25.3	4.5	Cr″–Cr′
1f	133.0	4.4	Iso–LC (SmA)
	82.0	12.0	LC (SmA)–Cr″
	36.4	9.3	Cr″–Cr′
2d	107.9	1.8	Iso–LC (SmA)
	60.0	18.7	LC (SmA)–Cr″
	4.4	8.0	Cr″–Cr′
2e	132.8	4.0	Iso–LC (SmA)
	71.4	19.7	LC (SmA)–Cr″
	28.9	6.6	Cr″–Cr′
2f	146.9	4.7	Iso–LC (SmA)
	76.5	18.3	LC (SmA)–Cr″
	46.7	15.5	Cr″–Cr′

[a] Transitions refer to the 2nd cooling cycles. Temperatures indicate the onset of each peak. The third transition of **1d** on cooling is not evaluable due to its small height. Abbreviations: Iso, isotropic phase; LC, liquid crystalline phase; SmA, smectic A phase; Cr″ and Cr′, crystalline solid-state.

Comparing the enthalpy values within the series with each other (**1d-f** and **2d-f**), they are quite alike for the second transitions, and no trend is visible. For the smaller peaks (first and third transition), the enthalpy values seem to rise, apart from a few exceptions (value of first transition of **1e** and third transition of **2e**). In general, the highest enthalpy values are calculated for the second transition of each salt. Since there are three relevant exothermic peaks in each DSC trace, it can be assumed that the samples exhibit LC phases or more than one crystalline phase. The first transition in the cooling cycle can be identified as the transition from the isotropic liquid into the liquid crystalline phase (I ⟶ LC) since the second transition in each DSC trace has too high enthalpy values to be a transition from a crystalline solid-state to another crystalline solid-state. The transition enthalpies of the second transitions, ranging from 12 to 19 kJ mol^{-1}, are smaller than the reference values from a liquid crystalline phase to a crystalline solid-state transition (30–50 kJ mol^{-1}), however, they are much higher than the values for transitions from LC to LC or LC to an isotropic liquid (4–6 kJ mol^{-1}) [23]. This indicates that the second transitions can be assigned to a transition from a liquid crystalline phase to a crystalline solid-state (LC ⟶ Cr″). The enthalpy of the third transition is smaller compared to the

second transition and led to the assumption that a transition from a crystalline solid-state to another crystalline solid-state (Cr″⟶ Cr′) takes place.

The salts were further analyzed by POM to identify and confirm the liquid crystalline phases. Two transitions could be observed during the POM analysis for each salt by heating and cooling the samples at 10 °C min^{-1}. The following discussion will concentrate on the cooling events. When cooling the samples from the isotropic liquid, a change from the dark isotropic liquid phase into a birefringent phase has been observed for every salt, whereby the new structure was formed very slowly over a wide temperature range. Furthermore, a second structure change has been observed when cooling the salts further, which was very fast. The first transition from the isotropic liquid into the birefringent mesophase (I ⟶ LC) is illustrated in the supporting information S10. The mesophase after a full transition is shown in Figure 2 for the salts **1d-f** and **2d-f,** showing typical liquid crystalline textures. The hypothesis, from the DSC traces, that the first transition refers to the I ⟶ LC transition and the second to a LC ⟶ Cr″ transition can be verified by the POM analysis (data reported in the supporting information S11 for LC ⟶ Cr″ transition). However, following the LC ⟶ Cr″ transition, no Cr″ ⟶ Cr′ transition could be observed by POM. As the mesophases are reversibly formed during heating and cooling, the compounds can be classified as enantiotropic ionic liquid crystals. The structure of the compounds likely leads to the conclusion that the perfluoroalkyl chains and the alkyl chains will segregate from one another, as previously observed for similar systems [10,15,16]. Indeed, the long perfluoroheptyl chain introduces a certain structural stiffness conferring stability to the thermotropic LC phase. Comparing the salts from this work with the previous work with only *N*-methylated pyridinium salts [10], we can assume that the additional alkyl chain in this compound tends to stress self-aggregation in the mesophase due to the van der Waals interactions between the molecules driving the formation of LC phases. As reported in previous studies, micro-segregation is involved in the formation of smectic-like phases [24]. By comparing the textures observed by POM of these salts to pictures from literature, it is reasonable to hypothesize a smectic A (SmA) phase for all the salts; in fact, the defects look like SmA bâtonnets growing into focal conic textures [25].

Discussing the mesophase range with respect to the structural variables, it can be clearly seen that the mesophase range increases with the increasing alkyl chain length within the series, as shown in Figure 3. By comparing the regioisomers with each other, salts **2d-f** have a wider mesophase range than the **1d-f** samples, indicating a higher stability of the liquid crystalline phase. The different behavior between the regioisomers can be explained by the different linkage of the pyridinium ring and the resulting effect of charge delocalization due to the distortion of the linearity. When the pyridinium ring is linked to the C(5) of the 1,2,4-oxadiazole (**2d-f**), the conjugation of the system increased compared to the pyridinium linked to the C(3) of the 1,2,4-oxadiazole (**1d-f**), resulting in a higher effect of charge delocalization for the compounds **2d-f**. The enhanced positive charge delocalization increases the size of the polar head and affects the extent of the charge dispersion favoring a higher anion mobility. This is supported by the lower transition temperatures for **2d-f** and thus the wider mesophase range.

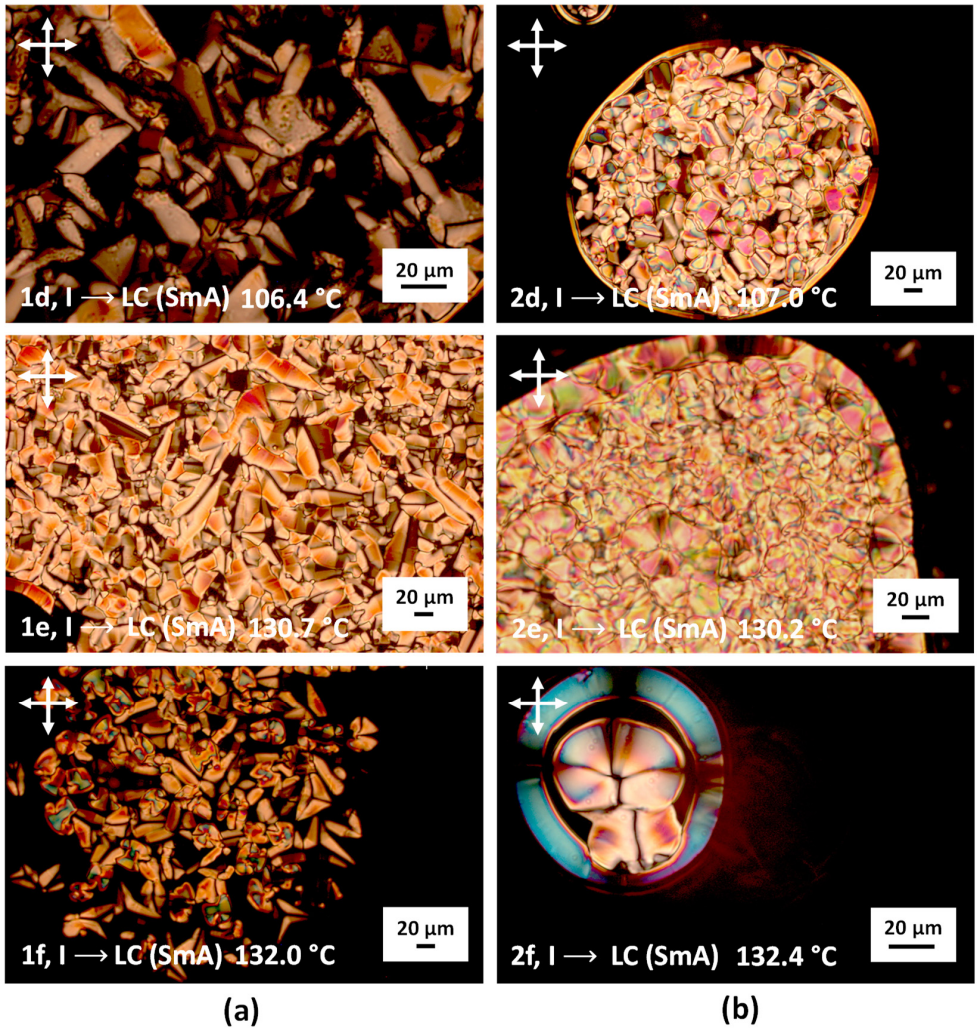

Figure 2. Optical textures of the salts (**a**) **1d** at 106.4 °C, **1e** at 130.7 °C, **1f** at 132.0 °C and (**b**) **2d** at 107.0 °C, **2e** at 130.2 °C, **2f** at 132.4 °C observed by polarized optical microscopy analysis under crossed polarizers showing the mesophase after the 1st transition from the isotropic liquid to the liquid crystalline phase (I ⟶ LC (SmA)) upon cooling with 10 °C min^{-1}. Abbreviation: I, isotropic phase; LC, liquid crystalline phase; SmA, smectic A phase.

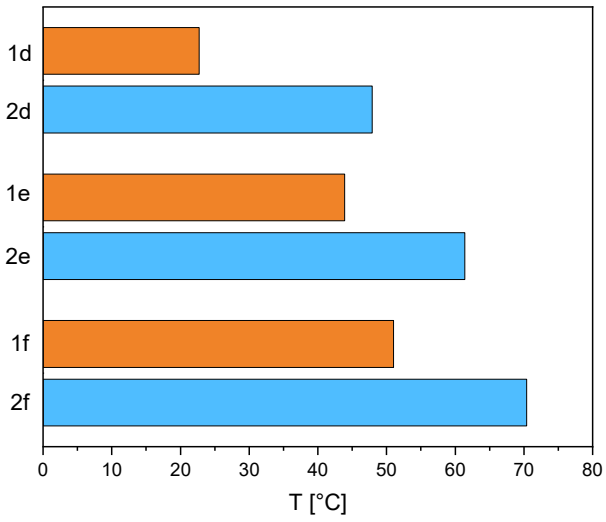

Figure 3. Comparison of the mesophase range of the salts **1d-f** and **2d-f**.

4. Conclusions

A series of 12 novel fluorinated heterocyclic salts containing an asymmetric 1,2,4-oxadiazole moiety connected through its C(5) or C(3) to an *N*-alkyl-pyridinium unit and a perfluoroheptyl chain as cation and iodide, bromide and bis(trifluoromethane)sulfonimide as counterions, has been synthesized. The physico-chemical properties have been studied by means of different techniques such as differential scanning calorimetry and polarized optical microscopy. The precursor salts containing iodide and bromide as counterions did not exhibit any liquid crystalline phase behavior—except for **2a**. However, after metathesis, the salts containing bis(trifluoromethane)sulfonimide as the counterion (**1d-f**, **2d-f**) can be classified as enantiotropic smectic ionic liquid crystals. The thermotropic behavior, in particular the mesophase range of these salts, is a function of the linkage of the pyridinium ring on the 1,2,4-oxadiazole C(3) or C(5) and the alkyl chain length. In fact, the compounds linked to the more conjugated part of the oxazolic part C(5) form a wider mesophase range with respect to the salts linked to C(3). Furthermore, it can be assessed that the mesophase range increases with increasing alkyl chain length. All salts showed a melting point lower than 100 °C.

We can conclude that these ILCs are promising candidates for innovative applications. In future studies, they will be investigated as components for smart materials, ion-conductive batteries, and dye-sensitized solar cells.

Supplementary Materials: The following are available online at https://www.mdpi.com/article/10.3390/app112110347/s1, ^{1}H-NMR spectra of **1**, **1a-c**, **2** and **2a-c** (S1–S8), Synthesis and analytical data for **1a'** (S9). Polarized optical microscopy images of **1d-f** and **2d-f** (S10 and S11).

Author Contributions: Conceptualization, I.P.; methodology, I.P.; formal analysis, M.S.W., G.L. and A.P.P.; investigation, M.S.W.; resources, A.P. and I.P.; data curation, M.S.W.; writing—original draft preparation, M.S.W.; writing—review and editing, M.S.; supervision, I.P. and M.S.; funding acquisition, I.P. All authors have read and agreed to the published version of the manuscript.

Funding: This research was funded by the University of Palermo, grant number FFR2019 to Ivana Pibiri.

Institutional Review Board Statement: Not applicable.

Informed Consent Statement: Not applicable.

Data Availability Statement: Raw data can be made available by the corresponding author.

Conflicts of Interest: The authors declare no conflict of interest.

References

1. Binnemanns, K. Ionic Liquid Crystals. *Chem. Rev.* **2005**, *105*, 4148–4204. [CrossRef] [PubMed]
2. Rizzo, C.; Marullo, S.; Campodonico, P.R.; Pibiri, I.; Dintcheva, N.T.; Noto, R.; Millan, D.; D'Anna, F. Self-Sustaining Supramolecular Ionic Liquid Gels for Dye Adsorption. *ACS Sustain. Chem. Eng.* **2018**, *6*, 12453–12462. [CrossRef]
3. Pibiri, I.; Pace, A.; Buscemi, S.; Causin, V.; Rastrelli, F.; Saielli, G. Oxadiazolyl-pyridines and perfluoroalkyl-carboxylic acids as building blocks for protic ionic liquids: Crossing the thin line between ionic and hydrogen bonded materials. *Phys. Chem. Chem. Phys.* **2012**, *14*, 14306–14314. [CrossRef]
4. Goossens, K.; Lava, K.; Bielawski, C.W.; Binnemans, K. Ionic Liquid Crystals: Versatile Materials. *Chem. Rev.* **2016**, *116*, 4643–4807. [CrossRef]
5. Kato, T. *Liquid Crystalline Functional Assemblies and Their Supramolecular Structures*; Springer: Berlin/Heidelberg, Germany, 2008; p. 151. ISBN 978-3-540-77866-0.
6. Yuan, F.; Chi, S.; Dong, S.; Zou, X.; Lv, S.; Bao, L.; Wang, J. Ionic liquid crystal with fast ion-conductive tunnels for potential application in solvent-free Li-ion batteries. *Electrochim. Acta* **2019**, *294*, 249–259. [CrossRef]
7. Ohtake, T.; Tanaka, H.; Matsumoto, T.; Kimura, M.; Ohta, A. Redox-driven molecular switches consisting of bis(benzodithiolyl)bithienyl scaffold and mesogenic moieties: Synthesis and complexes with liquid crystalline polymer. *J. Org. Chem.* **2014**, *79*, 6590–6602. [CrossRef]
8. Pibiri, I.; Pace, A.; Palumbo Piccionello, A.; Pierro, P.; Buscemi, S. Synthesis and Characterization of a Series of Alkyl-Oxadiazolylpyridinium Salts as Perspective Ionic Liquids. *Heterocycles* **2006**, *68*, 2653–2661. [CrossRef]
9. Pibiri, I.; Pace, A.; Buscemi, S.; Vivona, N.; Malpezzi, L. Designing Fluorous Domains. Synthesis of a Series of Pyridinium Salts Bearing a Perfluoroalkylated Azole Moiety. *Heterocylces* **2006**, *68*, 307–321. [CrossRef]

10. Lo Celso, F.; Pibiri, I.; Triolo, A.; Triolo, R.; Pace, A.; Buscemi, S.; Vivona, N. Study on the thermotropic properties of highly fluorinated 1,2,4-oxadiazolylpyridinium salts and their perspective applications as ionic liquid crystals. *J. Mater. Chem.* **2007**, *17*, 1201–1208. [CrossRef]
11. Saccone, M.; Cavallo, G.; Metrangolo, P.; Pace, A.; Pibiri, I.; Pilati, T.; Resnati, G.; Terraneo, G. Halogen bond directionality translates tecton geometry into self-assembled architecture geometry. *CrystEngComm* **2013**, *15*, 3102–3105. [CrossRef]
12. Haristory, D.; Tsiourvas, D. Novel Ionic Liquid-Crystalline Compounds Bearing Oxadiazole and Pyridinium Moieties as Prospective Materials for Optoelectronic Applications. *Chem. Mater.* **2003**, *15*, 2079–2083. [CrossRef]
13. Kraft, A.; Grimsdale, A.C.; Holmes, A.B. Electroluminescent Conjugated Polymers—Seeing Polymers in a New Light. *Angew. Chem. Int. Ed.* **1998**, *37*, 402–428. [CrossRef]
14. Riccobono, A.; Parker, R.R.; Whitwood, A.C.; Slattery, J.M.; Bruce, D.W.; Pibiri, I.; Pace, A. 1,2,4-Triazolium ions as flexible scaffolds for the construction of polyphilic ionic liquid crystals. *Chem. Commun.* **2018**, *54*, 9965–9968. [CrossRef]
15. Riccobono, A.; Lazzara, G.; Rogers, S.E.; Pibiri, I.; Pace, A.; Slattery, J.M.; Bruce, D.W. Synthesis and mesomorphism of related series of triphilic ionic liquid crystals based on 1,2,4-triazolium cations. *J. Mol. Liq.* **2021**, *321*, 114758. [CrossRef]
16. Abate, A.; Petrozza, A.; Cavallo, G.; Lanzani, G.; Matteucci, F.; Bruce, D.W.; Houbenov, N.; Metrangolo, P.; Resnati, G. Anisotropic ionic conductivity in fluorinated ionic liquid crystals suitable for optoelectronic applications. *J. Mater. Chem. A* **2013**, *1*, 6572–6578. [CrossRef]
17. Zama, I.; Gorni, G.; Borzatta, V.; Cassani, M.C.; Crupi, C.; Di Marco, G. Fluorinated imidazolium salts having liquid crystal characteristics. *J. Mol. Liq.* **2016**, *223*, 749–753. [CrossRef]
18. Buscemi, S.; Pace, A.; Palumbo Piccionello, A.; Macaluso, G.; Vivona, N.; Spinelli, D.; Giorgi, G. Fluorinated heterocyclic compounds. An effective strategy for the synthesis of fluorinated Z-oximes of 3-perfluoroalkyl-6-phenyl-2h-1,2,4-triazin-5-ones via a ring-enlargement reaction of 3-benzoyl-5-perfluoroalkyl-1,2,4-oxadiazoles and hydrazine. *J. Org. Chem.* **2005**, *70*, 3288–3291. [CrossRef]
19. Clapp, L.B. 1, 2, 4-Oxadiazoles. *Adv. Heterocycl. Chem.* **1976**, *20*, 65–116. [CrossRef]
20. Palumbo Piccionello, A.; Pace, A.; Buscemi, S. Rearrangements of 1,2,4-Oxadiazole: "One Ring to Rule Them All". *Chem. Heterocycl. Compd.* **2017**, *53*, 936–947. [CrossRef]
21. Chan, B.K.M.; Chang, N.; Grimmett, M.R. The synthesis and thermolysis of imidazole quaternary salts. *Aust. J. Chem.* **1977**, *30*, 2005–2013. [CrossRef]
22. Wasserscheid, P.; Welton, T. *Ionic Liquids in Synthesis*, 2nd ed.; WILEY-VCH Verlag GmbH & Co. KGaA: Weinheim, Germany, 2008; ISBN 978-3-527-31239-9.
23. Singh, S.; Dunmur, D.A. *Liquid Crystals: Fundamentals*; World Scientific Publishing Co Pte Ltd.: Singapore, 2002; pp. 58–59. ISBN 981-02-4250-3.
24. Guittard, F.; Taffin de Givenchy, E.; Geribaldi, S.; Cambon, A. Highly fluorinated thermotropic liquid crystals: An update. *J. Fluor. Chem.* **1999**, *100*, 85–96. [CrossRef]
25. Dierking, I. *Textures of Liquid Crystals*; Wiley-VCH Verlag GmbH & Co. KGaA: Weinheim, Germany, 2003; pp. 180–200. ISBN 3-527-30725-7.